Heliyon 10 (2024) e24778

Contents lists available at ScienceDirect

Heliyon

journal homepage: www.cell.com/heliyon

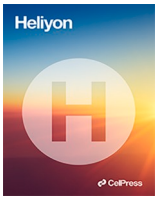

Research article

Anti-tumor effect and mechanism of the total biflavonoid extract from *S doederleinii* on human cervical cancer cells in vitro and in vivo

Shilan Lin [a,1], Zhijie Chen [a,1], Shaoguang Li [a], Bing Chen [a], Youjia Wu [a], Yanjie Zheng [a], Jianyong Huang [b,**], Yan Chen [c,***], Xinhua Lin [a], Hong Yao [a,*]

[a] *Department of Pharmaceutical Analysis, School of Pharmacy, Fujian Medical University, Fuzhou, China*
[b] *Department of Pharmacy, Fujian Medical University Union Hospital, Fuzhou, 350001, China*
[c] *Department of Medical Chemistry, School of Pharmacy, Fujian Medical University, Fuzhou, China*

ARTICLE INFO

Keywords:
Total biflavonoid extract of *S doederleinii*
Anti-cervical cancer effect
Caspase-dependent apoptosis
Autophagy

ABSTRACT

In this study, the therapeutic effect and possible mechanism of the total biflavonoid extract of *Selaginella doederleinii* Hieron (SDTBE) against cervical cancer were originally investigated in vitro and in vivo. First, the inhibition of SDTBE on proliferation of cervical cancer HeLa cells was evaluated, followed by morphological observation with AO/EB staining, Annexin V/PI assay, and autophagic flux monitoring to evaluate the possible effect of SDTBE on cell apoptosis and autophagy. Cell cycle, as well as mitochondrial membrane potential ($\Delta\Psi_m$), was detected with flow cytometry. Further, the apoptosis related protein expression and the autophagy related gene LC3 mRNA transcription level were analyzed by Western blot (WB) and real-time quantitative polymerase chain reaction (RT-qPCR), respectively. Finally, the anti-cervical cancer effect of the SDTBE was also validated in vivo in HeLa cells grafts mice. As results, SDTBE inhibited HeLa cells proliferation with the IC_{50} values of 49.05 ± 6.76 and 44.14 ± 4.75 μg/mL for 48 and 72 h treatment, respectively. The extract caused mitochondrial ΔΨ loss, induced cell apoptosis by upregulating Bax, downregulating Bcl-2, activating Caspase-9 and Caspase-3, promoting cell autophagy and blocking the cell cycle in G0/G1 phase. Furthermore, 100, 200, and 300 mg/kg SDTBE suppressed the growth of HeLa cells xenografts in mice with the mean inhibition rates, 25.3 %, 57.5 % and 62.9 %, respectively, and the change of apoptosis related proteins and microvascular density was confirmed in xenografts by immunohistochemistry analysis. The results show that SDTBE possesses anti-cervical cancer effect, and the mechanism involves in activating Caspase-dependent mitochondrial apoptosis pathway.

* Corresponding author.
** Corresponding author.
*** Corresponding author.
E-mail addresses: hjy8191@163.com (J. Huang), yanchen80801115@fjmu.edu.cn (Y. Chen), yauhung@126.com, hongyao@mail.fjmu.edu.cn (H. Yao).
[1] These authors contributed equally to this work.

https://doi.org/10.1016/j.heliyon.2024.e24778
Received 31 August 2023; Received in revised form 11 January 2024; Accepted 15 January 2024
Available online 17 January 2024

1. Introduction

Cervical cancer, primarily caused by high-risk human papillomavirus (HPV-HR) infection, stands as the fourth most prevalent woman cancer worldwide, and remains one of the primary causes of cancer associated mortality among women [1]. In recent years, the incidence rate of cervical cancer has risen significantly, and the patients tend to be younger. Early cervical cancer, regardless of surgery or radiotherapy, was satisfactory, and patient five-year survival rate was relatively high. However, for some high-risk cervical cancer due to large size of tumors and classification in the middle and late stage, prone to developing or experiencing disseminated tumor metastasis, the traditional surgical and radiotherapy efficacy of these patients are poor. Identifying efficient and low toxicity properties anti-cancer candidates is always a research hot spot in the fight against cervical cancer.

Anti-cancer applications of herbs have an extensive history. Herbs offer numerous benefits in managing cancer, including decreasing the toxicity of treatment, enhancing the quality of life, and/or augmenting the effectiveness of treatment [2]. Currently, it is still an attention spot for screening natural active ingredients [3,4], especially for anti-cancer candidates from herbal medicines [5]. *Selaginella doederleinii* Hieron, an anticancer Chinese herb medicine and belonging to the Selaginella genus of the Selaginellaceae family [6–8], has been recognized recently as a research topic by researchers due to its anti-cancer potentials [9–18]. According to the reports [7,8], *S. doederleinii* mainly contains bioflavonoid ingredients, which are the primary active ingredients in the herb and can be enriched in the ethyl acetate extract (SDTBE). Wang et al. [6] have reported that the SDTBE exhibits significant anti-tumor activity in vitro and has the ability to induce HepG2 cells apoptosis. The anti-tumor effects could be linked to a reduction in the gene expression of 5-LOX, COX-2, etc., and a decrease in the Bcl-2/Bax mRNA level ratio, the activation of caspase-3, and the suppression of survivin mRNA expression by the SDTBE. In our previous studies, the SDTBE demonstrated effective inhibitory effects on the proliferation of tumor cells, referring to lung cancer LLC, A549, and PC9 cells, as well as colorectal cancer HCT116 and HT29 cells [19,20]. Especially, it showed relatively high relevance (ranked top 5 in KEGG enrich-ment analysis) to human papillomavirus infection by proteomics study [21]. Thus, it is reasonable to assume that the SDTBE could have a beneficial effect against cervical cancer and should be considered for development as a potential agent against cervical cancer.

The present study aimed to further evaluate and validate the SDTBE's potential against cervical cancer, specifically regarding its potential role and mechanism in this disease. Therefore, the SDTBE was investigated originally in vitro on HeLa cells pertaining to cell proliferation, apoptosis, and the cell cycle. Furthermore, the underlying mechanism was studied for the first time through fluorescence microscopy, flow cytometry, Western blot (WB) and real-time quantitative polymerase chain reaction (RT-qPCR). The extract's anti-cervical cancer effect was confirmed with HeLa cells xenografts in mice through analyzing xenografts growth, MVD, and apoptosis-related proteins using immunohistochemistry.

2. Experimentals

2.1. Materials

S. doederleinii was obtained from a local drug store in Fuzhou, China, while the voucher specimens, identified by Prof. Hong Yao, were stored in the Phytochemistry Laboratory (Room 312) of Fujian Medical University (Fuzhou, China). The antibodies referring to

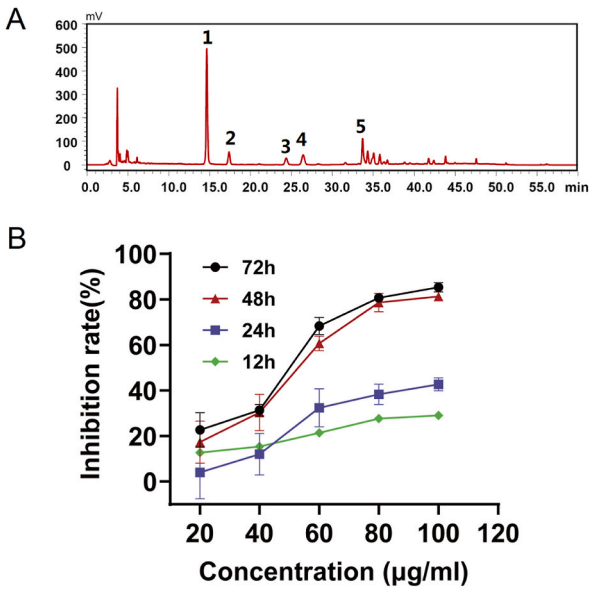

Fig. 1. (A) HPLC chromatogram of the extract: Peaks 1–5 are amentoflavone (22.9 %), robustaflavone (5.21 %), 2″,3″-dihydrogen-3′, 3‴-biapigenin (3.43 %), 3′,3‴- binaringenin (5.45 %), and (5) Delicaflavone (9.12 %). (B) Inhibitory effects of the SDTBE on the growth of HeLa cells in vitro.

caspase-3 (9665S), caspase-9 (7237S), Bcl-2 (2870S), and Bax (2774S) were provided by Cell Signaling Technology Inc. Acetonitrile and methanol were from Merck (HPLC grade; Darmstadt, Germany), and glacial acetic acid was obtained from Alad-din (Shanghai, China). A Milli-Q system (Bedford, MA) provided purified water.

2.2. Preparation of the SDTBE

The SDTBE was prepared in accordance with the aforementioned report [19]. To obtain the crude extract, the entire plant was extracted with 70 % ethanol, followed by reduced pressure evaporation to eliminate the ethanol. The concentrate was then resuspended with water and extracted sequentially with petroleum ether, dichloromethane, and ethyl acetate. Ultimately, the SDTBE was obtained by gathering the ethyl acetate extract, followed by analyzing the five main components, amentoflavone, robustaflavone, 2″, 3″-dihydrogen-3′, 3‴-biapigenin, 3′,3‴-binaringenin, and delicaflavone, via HPLC (Fig. 1A) by peak area normalization [20].

2.3. Cell culture

HeLa cells were purchased from National Collection of Authenticated Cell Cultures in China, and cultured with RPMI-1640 medium (HyClone, USA) containing 10 % FBS (Gibco, USA) and 1 % penicillin–streptomycin maintained in a humidified incubator with 5 % CO_2 at 37 °C. Cells were grown and passaged at 70 % confluence in culture flasks with trypsin-EDTA solution. After three generations, cells were harvested to conduct the next experiments.

2.4. MTT assays

The viability of cells was detected by a 3-(4,5-dimethylthiazol-2-yl)-2,5-diphe-nyltetrazolium bromide (MTT) method as per the instructions provided in a previous report [20]. Briefly, 5×10^3 HeLa cells were introduced into 96-well plates and incubated for 24 h. Subsequently, the cells were exposed to varying concentrations of SDTBE for either 12 h, 24 h, 48 h or 72 h. Afterwards, add 20 μL of 5 mg/mL MTT solution to each well and incubate at 37 °C for an additional 4 h.Next, discard the medium in the plate and add 150 μL DMSO to each well. Then, use a microplate reader to record the absorbance of each well at 570 nm. In the experiment, the SDTBE was initially dissolved in DMSO and then further diluted with the culture medium to achieve a final DMSO concentration of 0.1%.

2.5. Morphologic analysis

To assess the pattern of cell death induced by SDTBE, acridine orange/ethidium bromide (AO/EB) staining was conducted according to the literature [20,21]. In AO/EB assay, living cells usually exhibit uniform green fluorescence, while chromatin condensation and nuclear lysis, as well as dense, deeply stained yellow green particles, are visible in apoptotic cells. In addition, transmission electron microscope (FEI, TECNAI G2, USA) was used to observe autophagosomes in cells according to literature [20].

2.6. Adenovirus transinfecting assay

Adenovirus transinfecting was carried out in the light of the literature [20]. In brief, the HeLa cells were infected with 10 μL autophagy double labeled adenovirus carrying mRFP-GFP-LC3 for 24 h. Afterwards, the cells were interfered with the studied drugs in 10 % RPMI-1640 for 24 h, followed by observation using a confocal microscope (Olympus FV-1000).

2.7. Cell apoptosis observation

Cell apoptosis was observed by flow cytometry with the Annexin V-FITC/PI double staining with kits instruction (BD Biosciences, Franklin Lakes, NJ) according to the literature [21,22]. HeLa cells were exposed to varying concentrations of SDTBE (0, 50, 100, and 200 μg/mL) for 48 h. Afterwards, cells were gathered and washed with ice-cold PBS, followed by resuspending within 200 μL binding buffer at a cell count of 1×10^5 cells per milliliter. The samples were hatched with 5 μL of Annexin V-FITC and PI in dark for 15 min at ambient temperature. Afterwards, the cells were detected using flow cytometry. Three independent experiments were conducted in the study.

2.8. Mitochondrial membrane potential ($\Delta\Psi_m$) evaluation

Mitochondrial membrane potential evaluation was performed according to previous reports [21,23–25]. HeLa cells were cultured until they reached a fusion of 70 %, after which they were digested with trypsin and adjusted to a cell density of approximately 1×10^5/mL with 10 % RPMI-1640 medium. Drop 150 μL of the cell suspension onto the cover glass that is situated in a six-well plate. When the cells attached to the cover glass, the medium on top was removed, and SDTBE (0, 50, 100 or 200 μg/mL) in 10 % RPMI-1640 medium were added to each well, followed by incubation for 24 h in a 37 °C and 5 % CO_2 incubator. After intervention for 24 h, the culture medium containing the drugs was discarded. Subsequently, 1 mL of cell culture medium and 1 mL of JC-1 staining working solution were added, which were then thoroughly mixed. Following an incubation period of 20 min in a 37 °C and 5 % CO_2 incubator, the supernatant was promptly removed through centrifugation. After resuspended with 2 mL culture medium, the cells were observed under a fluorescence inverted microscope. Green fluorescence from JC-1 monomer was utilized to show the lost $\Delta\Psi_m$.

2.9. Cell cycle detection

The cell cycle was detected with PI staining as per the previous report [20]. Briefly, HeLa cells were interfered with SDTBE (0, 50, 100, or 200 μg/mL) for 48 h, followed by digestion with trypsin alone to prepare into a cell suspension with the aid of culture medium. After centrifugation at 1000 rpm for 5 min, the cells were washed with PBS, carefully resuspended by blowing 70 % ethanol precooled at 4 °C, and fixed for more than 2 h at 4 °C. Subsequently, the fixing solution was removed through centrifugation at 1000 rpm, and the remains were then washed with PBS, followed by the addition of PI and RNase A and incubating for 30 min in dark at ambient temperature. Ultimately, the cells were stored in an ice box, shielded from light, and analyzed within 1 h by flow cytometry.

2.10. Western blot assay

HeLa cells were lysed in RIPA lysis buffer on ice for 30min. Following centrifugation for 15 min at 12,000×*g* and 4 °C, the content of protein in the supernatant was estimated using a BCA protein determination kit (Beyotime, China). Protein samples were separated using 10 % SDS-PAGE and then transferred to a PVDF film (Millipore, USA). The films were incubated in 0.1 % Tris-buffered saline with Tween 20 (TBST) with 5 % non-fat dry milk at ambient temperature for 1 h, followed by an overnight incubation with primary antibodies of Bax, Caspase-3, Caspase-9, or β-tublin at 4 °C. Afterwards, the films were washed with 0.1 % TBST for three times, followed by incubation with HRP-conjugated secondary antibodies for 1 h at ambient temperature. An ECL system (Millipore, USA) was used to detect the immunoreactive bands.

2.11. RT-PCR assay

The RT-PCR assay was conducted in accordance with the aforementioned report [20]. In brief, total RNAs were extracted from the collected cells with TRIzol Reagent (Engreen, Beijing, China) following the manufacturer's guidelines. A spectrophotometer was used to determine the concentrations of RNA, which was then adjusted to a final concentration of 200 ng/μL. The adjusted RNA was then encountered with RT-PCR using the RevertAid Kit (Thermo Scientific) as per the manufacturer's instructions. The mRNA expression levels of β-actin and LC3 were measured with the primers as follows in Table 1.

2.12. In vivo anti-cervical cancer assay

The Animal Care and Ethics Committee of Fujian Medical University (Fuzhou, China) approved the animal care and examination protocols (Approval No. FJMU IACUC 2017–0005). The mice were kept at 25 ± 2 °C and a relative humidity of 55 ± 5 %, with a 12 h light/dark cycle, and were provided with standard mouse chow and water ad libitum.

Xenograft models were prepared via subcutaneously injecting 1×10^7 HeLa cells into the right flank region of four-week old male athymic nude mice, provided by Slake Experimental Animal Co., Ltd., Shanghai, China. When the average size of xenografts reached approximately 100 mm^3, the animals were randomly divided by five groups (n = 6 per group), namely the control, the positive, and the three treatment groups. The control (solvent) or treatment groups (100, 200, and 300 mg/kg SDTBE) were administered by gavage daily until sacrifice. The positive group was daily administrated 3 mg/kg cisplatin through mice tail vein, and this continued until the mice were sacrificed. Mice body weight and tumor size were recorded every two days. The tumor size was computed with the formula: tumor volume = length × $width^2/2$. After treatment for 14 days, the mice were killed via neck dislocation, and the tumors were collected, weighed, and photographed. The inhibition of tumor was calculated according to the equation, tumor suppression (%)=(1-T/C) × 100, where T refers to the average tumor weight of the treated group, while C indicates the average tumor weight of the control group.

Hematoxylin/Eosin (H&E) staining for tumor tissues was conducted as per a literature [20]. In brief, the tumors were secured in 10 % formalin, dehydrated through a gradient of alcohol, encased in paraffin, sectioned and dyed with H&E. Immunohistochemical staining was conducted in accordance with a previously published report [18], utilizing CD34, Caspase-3, Caspase-9, Bax and Bcl-2 antibodies. The cell membrane of vascular endothelial cells express CD34, which can be stained brown or brownish-black for the cell membrane. The immunohistochemical analysis of MVD was conducted using the following method: the single or several endothelial cells stained brown were counted as one blood vessel, and the blood vessels with lumen diameter more than the sum of eight red blood cell diameters were excluded. The number of microvessels in the three fields (× 200) under light microscope was randomly counted in each slice, and the average number was calculated as the MVD number of the slice. The positive staining markers of Caspase3, Caspase9, Bax and Bcl-2 were brown granules, which were mainly expressed in cytoplasm. Image-ProPlus 6.0 image analysis software ana-lyzes the integrated optical density (IOD) value in each picture, and the average value in three fields in each slice was calculated as the amount of these proteins expressed in the tissue.

Table 1
The forward and reverse primer sequences for RT-PCR assay.

	β-actin	LC3
forward	5′- CACCCAGCACAATGAAGATCAAGAT-3′	5′-AGCAAAATCCCGGTGATCATC-3′
reverse	5′-CCAGTTTTTAAATCCTGAGTCAAGC -3′	5′- GCCGGATGATCTTGACCAACT -3′

2.13. Statistical analysis

The data were showed as mean ± SD and analyzed statistically by PASW Statistics 18 statistical software. The T-test was utilized for inter-groups comparison and p value less than 0.05 was considered statistically significant.

3. Results

3.1. Anti-proliferation effects of SDTBE on HeLa cells

Fig. 1B demonstrates that SDTBE has the ability to curb the growth of HeLa cells in a dose- and time-dependent manner. Especially, for 48 and 72 h treatment, the inhibition of the extract on HeLa cells was more favorable than those for 12 and 24 h treatment. The IC_{50} values for 48 and 72 h treatment were 49.05 ± 6.76 and 44.14 ± 4.75 μg/mL, respectively.

3.2. Effect of SDTBE on HeLa cells apoptosis

Cells apoptosis status was examined with AO/EB staining cells in the light of the previous report [19]. AO can penetrate normal and early apoptotic cells with intact membranes, fluorescing green when bound to DNA. EB only enter cells with damaged membranes, such as late apoptotic and dead cells, emitting orange-red fluorescence when bound to concentrated DNA fragments or apoptotic bodies. Fig. 2A demonstrates that as the concentration of SDTBE increases, green fluorescence diminishes and orange fluorescence manifests, indicating the sequential occurrence of cell apoptosis by the AO/EB staining assay. To investigate further the inhibitory impact of SDTBE on HeLa cells, sub-diploid DNA-content and phospholipidserine (PS) externalization were assessed with FACS following staining with Annexin V-FITC/PI. Observing significant late apoptosis of HeLa cells for the treatment with SDTBE (50, 100, or 200 μg/mL) for 48 h, particularly in the medium and high doses (Fig. 2B), further confirmed that SDTBE has the ability to induce apoptosis in HeLa cells.

3.3. Effect of the SDTBE on HeLa cells autophagy

It was observed under transmission electron microscope that the membrane in normal HeLa cells was complete, as well as the organelle, nuclei and chromosomes in the cytoplasm were normal (Fig. 3A). After treating HeLa cells with 50 μg/mL SDTBE for 24 h,

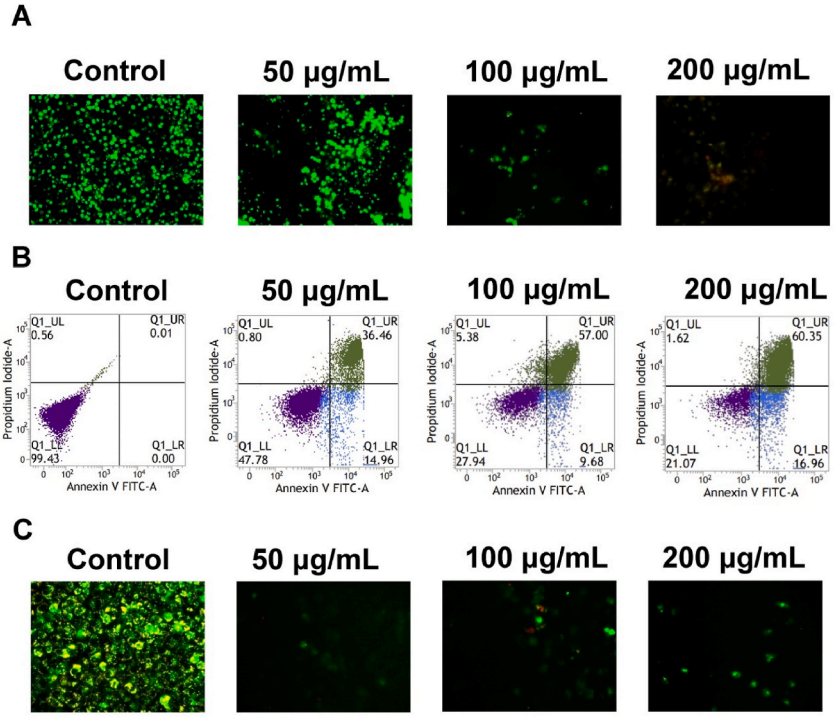

Fig. 2. (A) Morphological changes of HeLa cells treated with the SDTBE under fluorescence microscope. HeLa cells were incubated with the SDEAE (0, 50, 100, and 200 μg/mL) for 24 h and the cells were then collected and analyzed by AO/EB double-staining. (B) The apoptosis rate of HeLa cells induced by the SDTBE (0, 50, 100, and 200 μg/mL) for 48 h, stained with Annexin V-FITC/PI and analyzed by flow cytometry. (C) The effect of the SDTBE on $\Delta\Psi_m$ in HeLa cells.

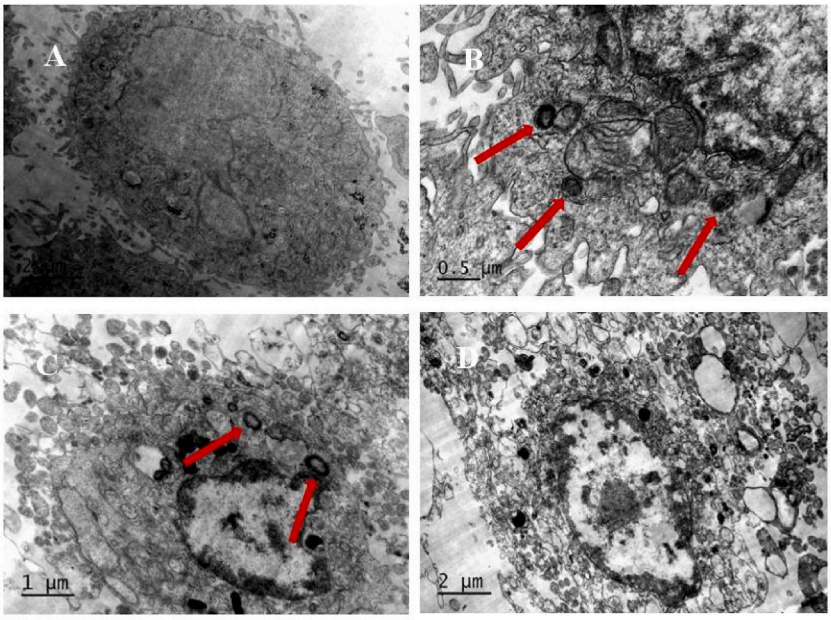

Fig. 3. Autophagosome formation of HeLa cells with the SDTBE treatment at (A) 0 μg/mL, (B) 50 μg/mL, (C) 100 μg/mL, and (D) 200 μg/mL.

the structure of double layer and multi-layer membrane appeared in the cytoplasm of the cells, and the autophagosome surrounding the undegraded organelle (such as ribosome) and cytoplasmic components (Fig. 3B). When the dosage of SDTBE increased to 100 μg/mL, the double layer and multi-layer structures still appeared in the cytoplasm of the cells, but partial necrosis occurred in the cells (Fig. 3C). When the dosage of SDTBE increased to 200 μg/mL, cell necrosis was severe, with a large number of vacuolar like structures and visible dissolution of nuclei and cytoplasm (Fig. 3D).

To validate further the autopahgic promotion effect of the SDTBE on HeLa cells, autophagy double labeled adenovirus tracing was performed. As shown in Fig. 4A, after treating HeLa cells with 50 μg/mL SDTBE, the autophagic flow increase, and as the concentration of SDTBE increase to 200 μg/mL, the fluorescence of green fluorescence protein (GFP) gradually weakens or even disappears, while the red fluorescence from red fluorescence protein (RFP) gradually increases (Fig. 4B, C and D), resulting in more red light spots. It can be determined that the level of autophagy flow is increased indeed for the SDTBE treatment on HeLa cells. In another word, the SDTBE treatment could induce excessive autophagy of HeLa cells, leading to autophagic cell death.

3.4. Effect of the SDTBE on $\Delta\Psi_m$

$\Delta\Psi_m$ was assessed with dye JC-1. As illustrated in Fig. 2C, the control group of HeLa cells produced intense yellow and green fluorescence. As the concentration of the extract increased, both yellow and green fluorescence diminished. Upon STBDE reaching a concentration of 200 μg/mL, the yellow fluorescence almost vanished, indicating that the cells had indeed experienced a loss of mitochondrial membrane potential due to apoptosis.

3.5. Effect of the SDTBE on cell cycle

The DNA of each phase of the cell cycle varies. Generally, G0 phase refers to the state in which cells are in a blocked state. To assess the inhibitory impact of SDTBE to HeLa cell proliferation, flow cytometry was employed to detect the cell cycle. As shown in Fig. 5A and B, with the dose increasing SDTBE from 50 to 200 μg/mL, the accumulation percentage in G0/G1 phase significantly increased from 45.12 ± 1.90 to 65.44 ± 0.68 % ($p < 0.01$, vs. 0 μg/mL), and meanwhile, S phase depletion was also observed significantly due to the SDTBE treatment ($p < 0.01$, vs. 0 μg/mL). The results mean the cell cycle was arrested at G0/G1 for the SDTBE treatment.

3.6. Effect of SDTBE on the apoptosis-associated proteins expression in HeLa cells

Mitochondrial pathway is an important endogenous pathway of apoptosis. Oligomerization of Bax promotes the activation of caspase apoptosis pathway by permeabilizing the outer mitochondrial membrane. When the levels of Bax and caspase series proteins, such as Caspase-9 and Caspase-3 are increased, it means the caspase apoptosis pathway could be activated in cells due to endogenous or exogenous stimuli. The levels of apoptosis-associated proteins, referring to Bax, Caspase-9, and Caspase-3 in HeLa cells were detected using WB assay. As shown in Fig. 6A–C, the SDTBE administration resulted in a dose-dependent increment in the protein expression levels of Bax, caspase-9, and caspase-3. These findings indicated that SDTBE promoted the apoptosis of HeLa cells by

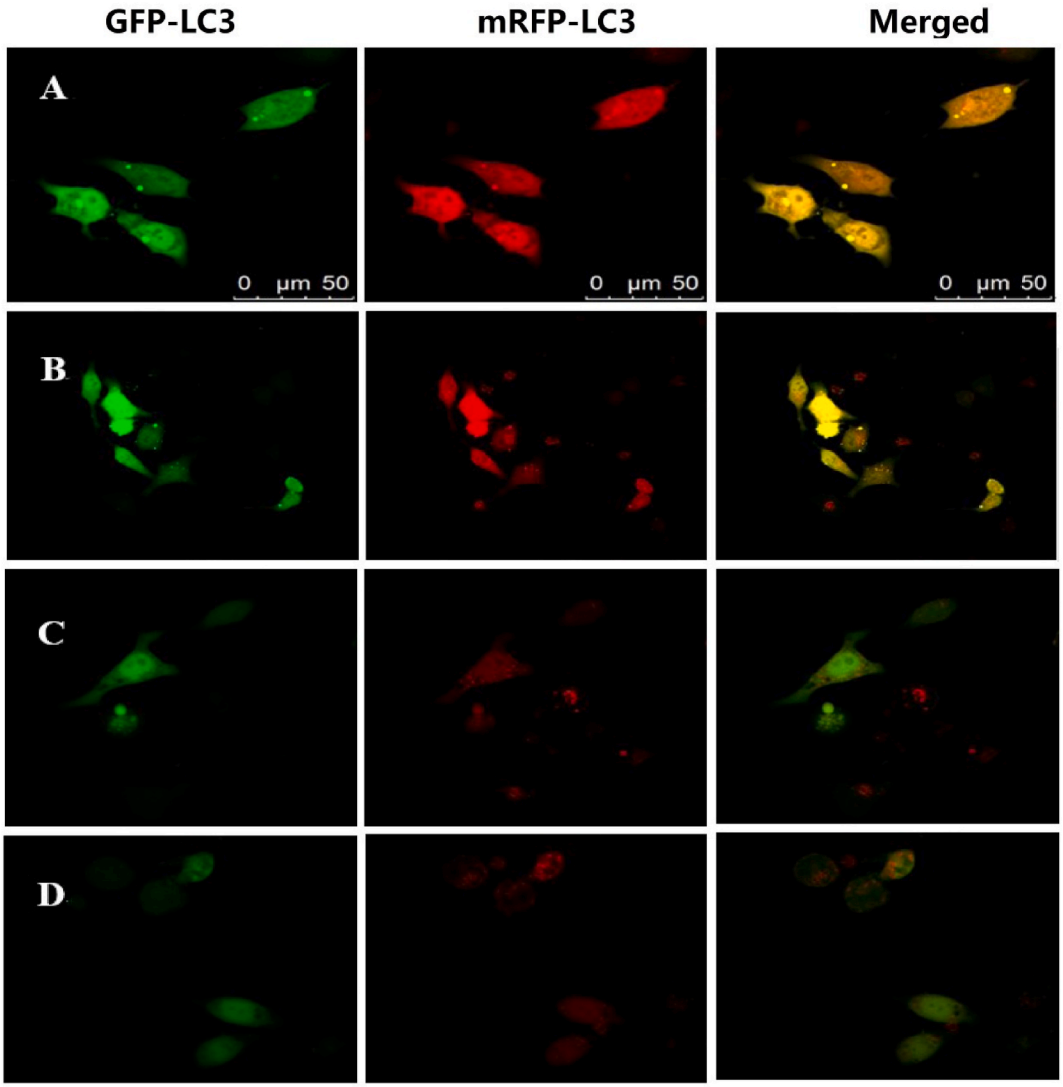

Fig. 4. HeLa cells were transfected with adenovirus expressing mRFP-GFP-LC3. (A) 0 μg/mL, (B) 50 μg/mL, (C) 100 μg/mL, and (D) 200 μg/mL SDTBE treatment.

enhancing the expression of Bax and activating the caspase-dependent signaling pathway *in vitro*.

3.7. Effect of the SDTBE on the level of LC3 mRNA in HeLa cells

As shown in Supplementary material S2, fluorescence quantitative PCR am-plification shows that the amplification curves of the internal reference gene β-actin and target gene LC3 are smooth and stable, and the fluorescence absorption spectrum curve is S-shaped, meeting the requirements of quantitative detection. It can be seen that as the concentration of SDTBE increases, the transcription level of autophagy related gene LC3 mRNA increases. All the treatment groups show significant statistical significance ($p < 0.01$, vs. the control group).

3.8. Anti-cervical cancer effect of the SDTBE in mice models

To confirm in vivo the cervical cancer growth inhibition effect of SDTBE, HeLa cell xenografted mice models were treated with the extract at a dose of 100, 200, or 300 mg/kg per day via gavage administration. After the treatment experiment, the xenografts were stripped and weighted. Under the naked eye, the tumor tissue was quasi-circular, hard, with clear boundary, and had capillary growth on the surface (Fig. 7A). When compared to the negative control group, the tumor body was observably smaller in the medium and high dose groups, as well as in the cisplatin-positive drug group ($p < 0.05$). Additionally, the capillary network on the surface of the tumor tissue was also observed to be reduced. The average weight and volume of the transplanted tumor in the three treatment groups

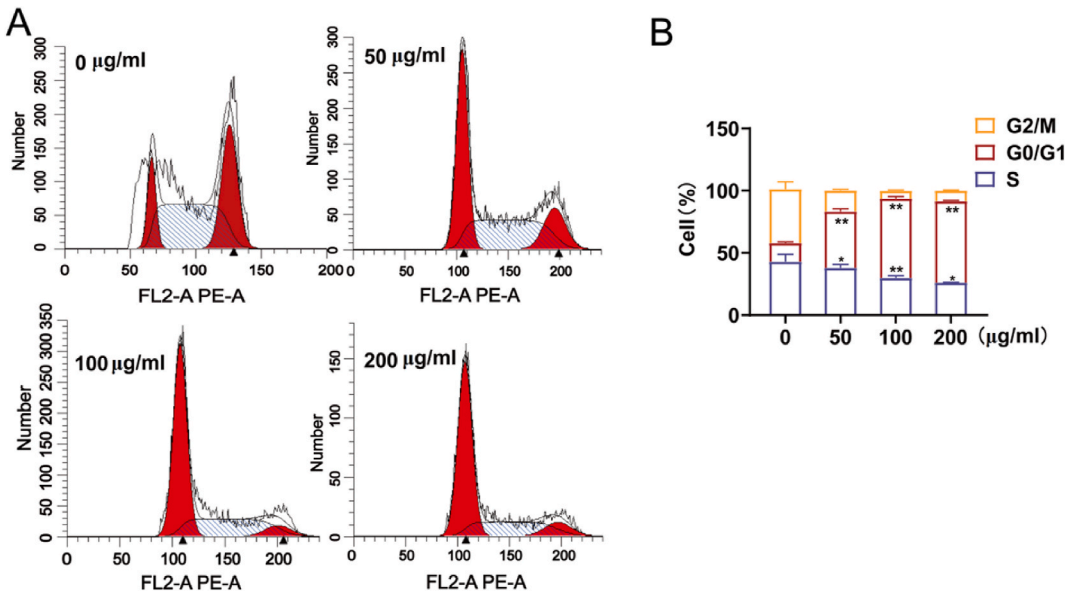

Fig. 5. Effect of the SDTBE on cell cycle in HeLa cells. (A) Flow cytometry graphs for cells treated with the extract (0, 50, 100, and 200 μg/mL) for 24 h, stained with PI and analyzed by. (B) Cell cycle phase proportions for the treatment of the different concentrations of extract. Data are presented as means ± SD (n = 3). *p < 0.05 and **p < 0.01, vs. the controls.

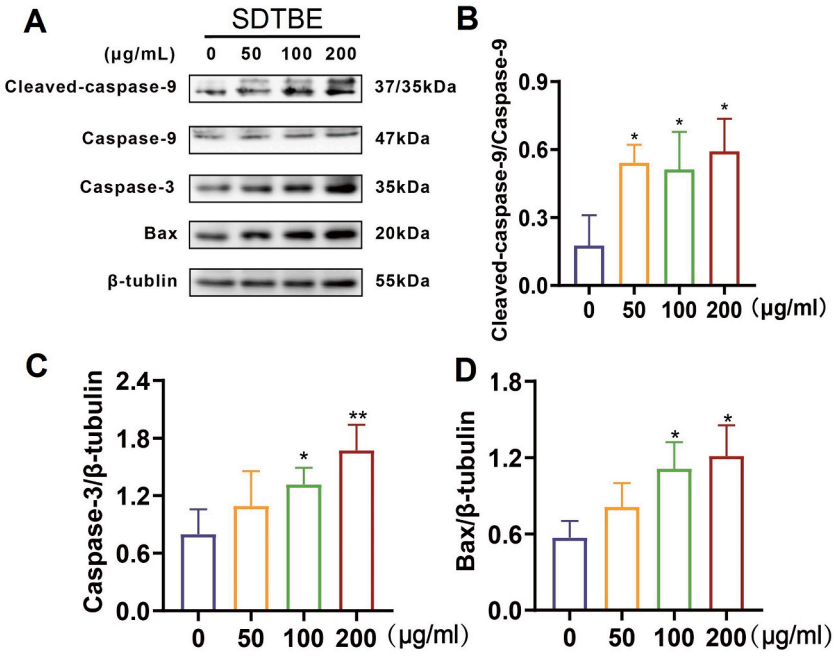

Fig. 6. Effects of the SDTBE on caspase 9/3 and Bax in HeLa cells. (A) WB assay bands for the treatment of different concentration of the SDTBE. Full, non-adjusted blot images are provided in Supplementary material S1. (B), (C) and (D) represent the histographs of the relative expression ratios of Cleaved-caspase-9/Caspase-9, Caspase-3/β-tubulin and Bax/β-tubulin, respectively for the treatment of different concentration of the SDTBE in the cells. *p < 0.05 and **p < 0.01, vs. the controls. β-tublin was used as an internal control.

were significantly decreased (p < 0.01, vs. control group) (Fig. 7B and C). The inhibitory effect of SDTBE on the HeLa cells xenografts presents a dose-dependent manner, and the mean inhibition rates were 25.3 %, 57.5 % and 62.9 % in low, medium and high dose groups, respectively.

H&E staining demonstrated that the tumor cells in the control group grow well and the tumor cells in tumor tissue are densely arranged (Fig. 7D). In the treatment groups, the density of tumor cells is significantly reduced with the increasing doses of the SDTBE,

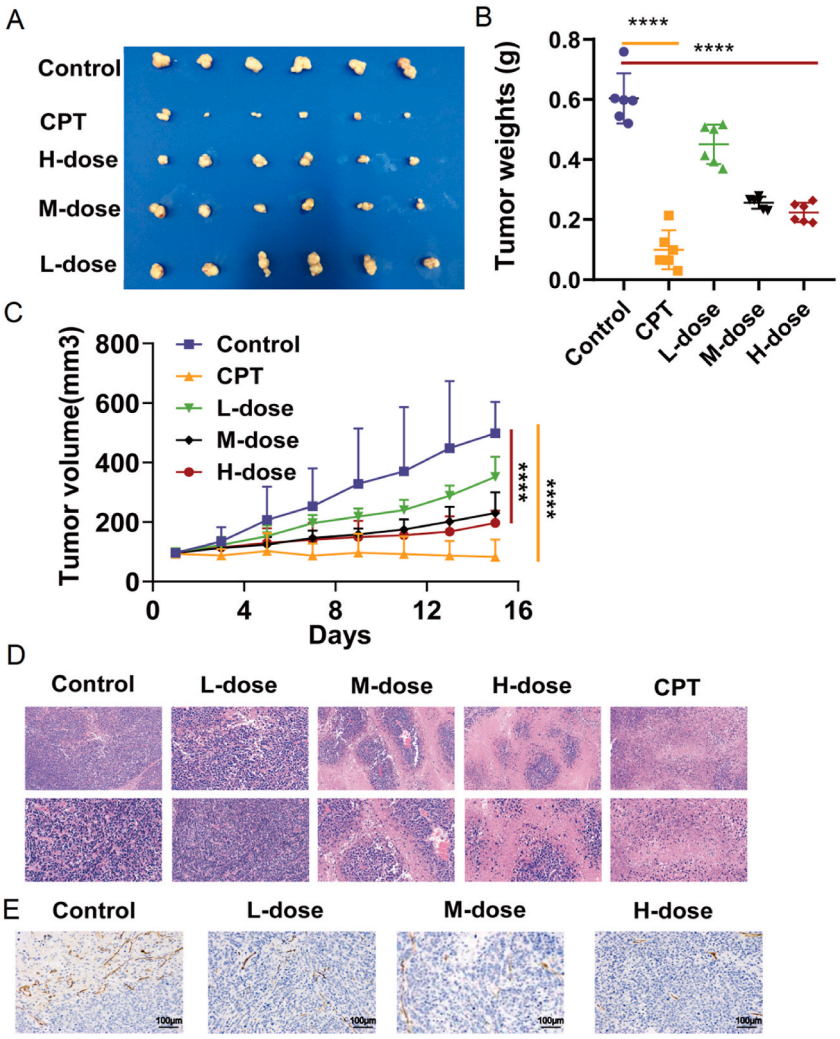

Fig. 7. Effect of the SDTBE on xenografts growth in mice. (A) Tumor volume, (B) tumor size, (C) tumor weight, (D) HE staining and (E) CD34 staining. Data are expressed as means ± SE, n = 6 mice per group. *p < 0.05 and **p < 0.01, vs. the control group.

indicating that the tumor growth is suppressed dose-dependently by the extract.

CD34 is specifically expressed in the cytoplasm of vascular endothelial cells, and can be stained as brown yellow particles. As shown in Fig. 7E, the microvessels were mainly distributed at the edge of the tumor tissue. The microvessel counts in each group are listed in Table 2. It indicates that the MVD counts of the HeLa cells xenografts in mice gradually decline as the SDTBE dose increases. The MVD count in both of the high and medium dose groups are notably different from that in the control group, with values of 10.44 ± 2.41 and 12.67 ± 0.33, respectively. These findings indicate a statistically significant difference ($p = 0.03$ and 0.015, respectively for high and medium dose groups vs. control group). As illustrated in Fig. 8A and B, the expression levels of anti-apoptotic related protein, Bax, pro-apoptosis related proteins, Caspase-9 and Caspase-3, are upregulated in the treatment groups ($p < 0.05$, vs. the control group). These results suggest that SDTBE may effectively suppress the growth of HeLa cells xenografts in mice by regulating the expression of

Table 2
MVD count of xenografts tumor in each group (n = 6, mean ± SD).

Group	MVD count
Control	26.44 ± 6.19
L-dose	17.78 ± 4.76
M-dose	12.67 ± 0.33*
H-dose	11.67 ± 2.41*

Compared with control group, *p<0.05.

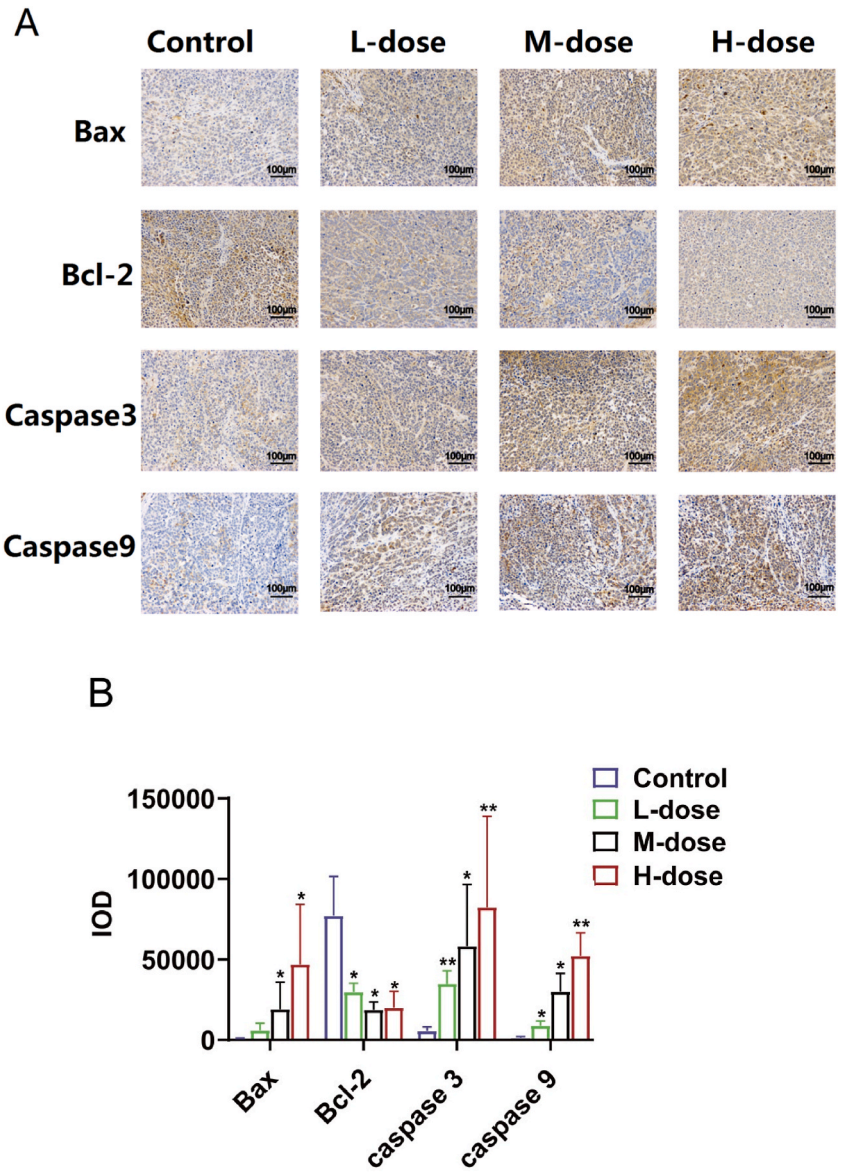

Fig. 8. Effects of the SDTBE on the expression of the apoptosis associated proteins in HeLa cells xenografts in mice. (A) the positive staining of Caspase3, Caspase9, and Bax and Bcl-2 proteins; (B) the integrated optical density (IOD) values of each protein expression. Data are expressed as means ± SE, n = 6 per group. *p < 0.05 and **p < 0.01, vs. the control group.

apoptosis-related proteins, suppressing the neovascularization in xenografts tumors, and decreasing the proliferation activity of the tumors.

4. Discussion

Studies have found that many biflavones play an anti-tumor role by inducing apoptosis and/or autophagic cell death of tumor cells. For example, the biflavone Hinokiflavone suppresses the growth of esophageal squamous cell carcinoma by regulating PI3K/AKT/mTOR signal pathway to induce apoptosis [26]. Delicaflavone plays an important role in preventing NSCLC, colon cancer and cervical cancer by activating mitochondrial dependent Caspase signal pathway and inhibiting MAPK and PI3K/Akt/mTOR signal pathway [27,28]. Isoinkgetin is a potential CDK6 inhibitor, which can inhibit the activity of SLC2A1/GUT1 enhancer and induce autophagic death of liver cancer cells [29]. Amentoflavone can inhibit E7 expression, block cell cycle in sub-G1 phase, and induce apoptosis of human cervical cancer cells through mitochondrial pathway [30]. SDTBE is considered to have broad-spectrum anticancer activity because it mainly contains such biflavones as Delicaflavone and Amentoflavone. Previous studies have confirmed that SDTBE has anti-hepatoma, anti-lung cancer, anti-colon cancer and other effects. This paper further studied the growth inhibition of SDTBE on human cervical

cancer HeLa cells in vitro and in vivo, in order to expand the anticancer spectrum of SDTBE for the sake of its drug development. MTT experiment confirmed that SDTBE inhibited the proliferation of human cervical cancer HeLa cells in vitro in a dose and time dependent manner, which suggests that SDTBE has good anti-cervical cancer activity.

Based on a previous research report [21], it is reasonable to consider that the inhibition of SDTBE on cervical cancer cell proliferation could be related to cell apoptosis and autophagy. AO and EB staining is considered to be a suitable way for qualitative assessment of cell apoptosis [19]. In this study, AO/EB staining results showed that green fluorescence attenuated and orange fluorescence appeared for the extract treatment, suggesting that SDTBE induced cell apoptosis, which was further confirmed by the annexin V-FITC/PI staining results. Meanwhile, autophagosomes were observed by transmission electron microscope in SDTBE treated cells, suggesting that SDTBE also induced cell autophagy, which was further confirmed by autophagy double labeled adenovirus tracing assay.

The unlimited proliferation of malignant tumors is closely related to the imbalance of cell cycle period [19,20]. There are two most important phases in cell cycle, namely G1/S and G2/M stages. These two phases are in a period of complex and active molecular level changes, easily affected by environmental condition and drug inter-vention, and they play important roles in controlling tumor growth. In this study, SDTBE treatment significantly prolonged the G0/G1 and S phases in HeLa cells, suggesting that SDTBE blocked the cell cycle process of G0/G1 and S phases, which once again confirmed the anti-HeLa cell proliferation effect of the extract.

Tumor cell apoptosis mainly involves in three pathways, including the cell surface death receptor-mediated pathway, the endoplasmic reticulum pathway, and the mitochondrial apoptosis pathway. The mitochondrial apoptosis pathway is the central mechanism of apoptosis induction [31], and it is mediated by Bcl-2 family proteins that possess either anti-apoptotic or pro-apoptotic characteristics, including Bcl-2 and Bax [32]. The $\Delta\Psi_m$ loss is known to cause the cytochrome C release, which in turn triggers the formation of an apoptotic complex, as well as Caspase-9. After activation of Caspase-9, it next activates Caspase-3, leading to the production of cleaved Caspase-3, ultimately accomplishing cell apoptosis [33]. The Caspase-3 activation signifies that apoptosis has entered an irreversible stage. In this study, it was observed that SDTBE caused the $\Delta\Psi_m$ loss in HeLa cells, thereby leading to the cytochrome C release. The subsequent WB assay revealed that SDTBE significantly increased the expression of Bax and decreased the caspase-9 and -3 expression levels. Meanwhile, the RT-PCR assay revealed a rise in LC3 levels in HeLa cells with the increasing SDTBE, thereby further confirming that SDTBE indeed stimulates autophagy in HeLa cells.

By targeting the CD34 surface of endothelial cells, immunohistochemical quantification of tumor microvessels can be performed, which can be denoted as MVD counts [19]. The MVD counts indicate that SDTBE has a significant ability to suppress the growth of HeLa cell xenografts by decreasing microvessel density. This suggests that the SDTBE inhibited tumor angiogenesis in vivo, which could be another crucial factor contributing to the extract's anticervical cancer effects.

To summarize, the SDTBE displays an advantageous effect against cervical cancer, and its mechanism involves hindering the cell cycle at G0/G1 and S phases, reducing the mitochondrial membrane potential, suppressing tumor angiogenesis, activating the Caspase-dependent mitochondrial apoptosis pathway, promoting cell autophagy, and ultimately inducing the death of cervical cells. In conclusion, the SDTBE could be considered a chemotherapeutic candidate for the treatment of cervical cancer.

Ultimately, the present study still remains a few limitations. In fact, this study only detected the effect of SDTBE on LC3 mRNA levels in HeLa cells. In order to confirm the autophagy induction effect of SDTBE in HeLa cells, further quantitation of the protein expression levels of LC3I and LC3II is needed, and attention should have been paid to the mechanism of SDTBE inducing autophagy in HeLa cells, which of course should be explored in the future experiments.

Ethical statement

All animal experiments were approved by the Institutional Animal Care and Use Committee of Fujian Medical University (Approval No. FJMU IACUC 2017–0005).

Data availability statement

Data will be made available on request.

CRediT authorship contribution statement

Shilan Lin: Writing – original draft, Investigation, Data curation. **Zhijie Chen:** Investigation. **Shaoguang Li:** Resources, Funding acquisition. **Bing Chen:** Resources. **Youjia Wu:** Resources. **Yanjie Zheng:** Funding acquisition. **Jianyong Huang:** Funding acquisition, Conceptualization. **Yan Chen:** Conceptualization. **Xinhua Lin:** Resources. **Hong Yao:** Writing – review & editing, Supervision, Resources, Project administration, Funding acquisition, Conceptualization.

Declaration of competing interest

The authors declare that they have no known competing financial interests or personal relationships that could have appeared to influence the work reported in this paper.

Acknowledgement

This study was supported by the Key project supported by the Natural Science Foundation of Fujian province, China (grant numbers 2021J02033), the Fujian Provincial Natural Science Foundation (2021J01683 and 2021J01686), the joint Funds for the Innovation of Science and Technology, Fujian Province (2019Y9068) and Fujian provincial health technology project (2021GGA011).

Appendix A. Supplementary data

Supplementary data to this article can be found online at https://doi.org/10.1016/j.heliyon.2024.e24778.

References

[1] H. Sung, J. Ferlay, R.L. Siegel, M. Laversanne, I. Soerjomataram, A. Jemal, F. Bray, Global cancer statistics 2020: GLOBOCAN estimates of incidence and mortality worldwide for 36 cancers in 185 countries, Ca-Cancer J Clin 71 (2021) 209–249.
[2] E. Chu, Wedding rigorous scientific methodology and ancient herbal wisdom to benefit cancer patients: the development of PHY906, Oncology-Basel 32 (2018) e20–e27.
[3] X.J. Jiang, Y.H. Lin, Y.L. Wu, C.X. Yuan, X.L. Lang, J.Y. Chen, C.Y. Zhu, X.Y. Yang, Y. Huang, H. Wang, C.S. Wu, Identification of potential anti-pneumonia pharmacological components of *Glycyrrhizae Radix* et Rhizoma after the treatment with Gan an He Ji oral liquid, J Pharm Anal 12 (2022) 839–851.
[4] X.Y. Lu, Y.Y. Jin, Y.Z. Wang, Y.L. Chen, X.H. Fan, Multimodal integrated strategy for the discovery and identification of quality markers in traditional Chinese medicine, J Pharm Anal 12 (2022) 701–710.
[5] A.G. Atanasov, S.B. Zotchev, V.M. Dirsch, , the International Natural Product Sciences Taskforce, C.T. Supuran, Natural products in drug discovery: advances and opportunities, Nat. Rev. Drug Discov. 20 (2021) 200–216.
[6] J. Wang, J. Li, P. Zhao, W.-T. Ma, X.-H. Feng, K.-L. Chen, Antitumor activities of ethyl acetate extracts from *Selaginella doederleinii* Hieron in vitro and in vivo and its possible mechanism, Evid-based Compl Alt 10 (2014) 529.
[7] S. Li, M. Zhao, Y. Li, Y. Sui, H. Yao, L. Huang, X. Lin, Preparative isolation of six anti-tumour biflavonoids from Selaginella doederleinii Hieron by high-speed counter-current chromatography, Phytochem. Anal. 25 (2014) 127–133.
[8] S. Li, H. Yao, M. Zhao, Y. Li, L. Huang, X. Lin, Determination of seven biflavones of *Selaginella doederleinii* by high performance liquid chromatography, Anal. Lett. 46 (2013) 2835–2845.
[9] F. Zhang, S. Li, C. Liu, K. Fang, Y. Jiang, J. Zhang, J. Lan, L. Zhu, H. Pang, G. Wang, Rapid screening for acetylcholinesterase inhibitors in *Selaginella doederleinii* Hieron by using functionalized magnetic Fe_3O_4 nanoparticles, Talanta 243 (2022) 123284.
[10] B. Chen, H. Luo, W. Chen, Q. Huang, K. Zheng, D. Xu, S. Li, A. Liu, L. Huang, Y.J. Zheng, Pharmacokinetics, tissue distribution, and human serum albumin binding properties of delicaflavone, a novel anti-tumor candidate, Front. Pharmacol. 12 (2021) 761884.
[11] B. Chen, X. Wang, Y. Zhang, K. Huang, H. Liu, D. Xu, S. Li, Q. Liu, J. Huang, H. Yao, Improved solubility, dissolution rate, and oral bioavailability of main biflavonoids from *Selaginella doederleinii* extract by amorphous solid dispersion, Drug Deliv. 27 (2020) 309–322.
[12] B. Chen, D. Xu, Z. Li, Y. Jing, L. Lin, S. Li, L. Huang, X. Huang, A. Liu, X. Lin, Tissue distribution, excretion, and interaction with human serum albumin of total bioflavonoid extract from *Selaginella doederleinii*, Front. Pharmacol. 13 (2022) 849110.
[13] M.Y. Chen, S.S. Wang, H.T. Cheng, D.R. Wan, R.M. Lu, X.Z. Yang, G.-I. Seladoeflavones, Three new flavonoids from *Selaginella doederleinii* hieron, ChemistrySelect 7 (2022) e202202242.
[14] G. Li, X. Gao, G. Qin, J. Lei, Y. Jiang, L. Linghu, C. Zhang, J. Zhang, Y. Wang, M.J. Wang, Purification of biflavonoids from *Selaginelladoe derleinii* Hieron by special covalent organic polymers material, J. Chromatogr. A 1668 (2022) 462920.
[15] S. Li, Z. Li, H. Li, C. Zhong, K. Huang, B. Chen, L. Huang, X. Lin, Q. Liu, H. Yao, Synthesis, biological evaluation, pharmacokinetic studies and molecular docking of 4″-acetyl-delicaflavone as antitumor agents, Bioorg. Chem. 120 (2022) 105638.
[16] F.W. Muema, Y. Liu, Y. Zhang, G. Chen, M. Guo, Flavonoids from *Selaginella Doederleinii* Hieron and Their Antioxidant and Antiproliferative Activities, Antioxidants-Basel11, 2022, p. 1189.
[17] S. Wang, D. Wan, W. Liu, X. Kang, X. Zhou, F. Sefidkon, M.M.Z. Hosseini, T. Zhang, X. Pan, X. Yang, Biflavonoid-rich extract from *Selaginella doederleinii* Hieron against throat carcinoma via Akt/Bad and IKKβ/NF-κB/COX-2 pathways, Pharmaceuticals 15 (2022) 1505.
[18] H.B. Yao, Chen, Y. Zhang, H. Ou, Y. Li, S. Li, P. Shi, X. Lin, Analysis of the total biflavonoids extract from *Selaginella doederleinii* by HPLC-QTOF-MS and its in vitro and in vivo anticancer effects, Molecules 22 (2017) 325.
[19] Y. Sui, S. Li, P. Shi, Y. Wu, Y. Li, W. Chen, L. Huang, H. Yao, X. Lin, Ethyl acetate extract from *Selaginella doederleinii* Hieron inhibits the growth of human lung cancer cells A549 via caspase-dependent apoptosis pathway, J Ethnopharmcol 190 (2016) 261–271.
[20] S. Li, X. Wang, G. Wang, P. Shi, S. Lin, D. Xu, B. Chen, A. Liu, L. Huang, X. Lin, Ethyl acetate extract of *Selaginella doederleinii* hieron induces cell autophagic death and apoptosis in colorectal cancer via PI3K-Akt-mTOR and AMPKα-signaling pathways, Front. Pharmacol. 11 (2020) 565090.
[21] D. Xu, X. Wang, D. Huang, B. Chen, X. Lin, A. Liu, J.Y. Huang, Disclosing targets and pharmacological mechanisms of total bioflavonoids extracted from Selaginella doederleinii against non-small cell lung cancer by combination of network pharmacology and proteomics, J. Ethnopharmacol. 286 (2022) 114836.
[22] M.S. Tousi, H. Sepehri, S. Khoee, M.M. Farimani, L. Delphi, F. Mansourizadeh, Evaluation of apoptotic effects of mPEG-b-PLGA coated iron oxide nanoparticles as a eupatorin carrier on DU-145 and LNCaP human prostate cancer cell lines, J Pharm Anal 11 (2021) 108–121.
[23] Y.Q. Song, G.D. Li, D. Niu, F. Chen, S.Z. Jing, V.K.W. Wong, W.H. Wang, C.H. Leung, A robust luminescent assay for screening alkyladenine DNA glycosylase inhibitors to overcome DNA repair and temozolomide drug resistance, J Pharm Anal 13 (2023) 514–522.
[24] Y.Y. Wang, L. Li, X.J. Liu, Q.F. Miao, Y. Li, M.R. Zhang, Y.S. Zhen, Development of a novel multi-functional integrated bioconjugate effectively targeting K-Ras mutant pancreatic cancer, J Pharm Anal 12 (2022) 232–242.
[25] L.L. Qu, Y.N. Liu, J.J. Deng, X.X. Ma, D.D. Fan, Ginsenoside Rk3 is a novel PI3K/AKT-targeting therapeutics agent that regulates autophagy and apoptosis in hepatocellular carcinoma, J Pharm Anal 13 (2023) 463–482.
[26] J. Guo, S. Zhang, J. Wang, P. Zhang, T. Lu, L. Zhang, Hinokiflavone inhibits growth of esophageal squamous cancer by inducing apoptosis via regulation of the PI3K/AKT/mTOR signaling pathway, Front. Pharmacol. 12 (2022) 127.
[27] W. Yao, Z. Lin, G. Wang, S. Li, B. Chen, Y. Sui, J. Huang, Q. Liu, P. Shi, X. Lin, Delicaflavone induces apoptosis via mitochondrial pathway accompanying G2/M cycle arrest and inhibition of MAPK signaling cascades in cervical cancer HeLa cells, Phytomedicine 62 (2019) 152973.
[28] W. Yao, Z. Lin, P. Shi, B. Chen, G. Wang, J. Huang, Y. Sui, Q. Liu, S. Li, X. Lin, Delicaflavone induces ROS-mediated apoptosis and inhibits PI3K/AKT/mTOR and Ras/MEK/Erk signaling pathways in colorectal cancer cells, Biochem. Pharmacol. 171 (2020) 113680.
[29] J. Yao, S. Tang, C. Shi, Y. Lin, L. Ge, Q. Chen, B. Ou, D. Liu, Y. Miao, Q. Xie, Isoginkgetin, a potential CDK6 inhibitor, suppresses SLC2A1/GLUT1 enhancer activity to induce AMPK-ULK1-mediated cytotoxic autophagy in hepatocellular carcinoma, Autophagy 19 (2023) 1221–1238.
[30] S. Lee, H. Kim, J.-W. Kang, J.-H. Kim, D.H. Lee, M.-S. Kim, Y. Yang, E.-R. Woo, Y.M. Kim, J.J. Hong, The biflavonoid amentoflavone induces apoptosis via suppressing E7 expression, cell cycle arrest at sub-G1 phase, and mitochondria-emanated intrinsic pathways in human cervical cancer cells, J. Med. Food 14 (2011) 808–816.

[31] P.T. Daniel, Dissecting the pathways to death, Leukemia 14 (2000) 2035–2044.
[32] J.M. Adams, Ways of dying: multiple pathways to apoptosis, Genes develop 17 (2003) 2481–2495.
[33] H. Zou, Y. Li, X. Liu, X.J. Wang, An APAF-1· cytochrome c multimeric complex is a functional apoptosome that activates procaspase-9, J. Biol. Chem. 274 (1999) 11549–11556.